Nonlinear flux-line dynamics in vanadium films with square lattices of submicron holes

V. Metlushko, U. Welp, and G. W. Crabtree

MSD, Argonne National Laboratory, Argonne, Illinois 60439-4845

Zhao Zhang and S. R. J. Brueck

University of New Mexico, Albuquerque, New Mexico 87131

B. Watkins and L. E. DeLong

University of Kentucky, Lexington, Kentucky 40506-0055

B. Ilic, K. Chung, and P. J. Hesketh

EECS, University of Illinois at Chicago, Chicago, Illinois 60607

Commensurability effects between the superconducting flux-line lattice and a square lattice (period $d = 1$ μm) of submicron holes (diameter $D = 0.4$ μm) in 1500 Å vanadium films were studied by atomic-force microscopy, dc magnetization, ac susceptibility, magnetoresistivity, and I-V measurements. Peaks in the susceptibility and critical current at matching fields are found to depend nonlinearly upon the value of external ac field or current, as well as the inferred symmetry of the flux-line lattice. [S0163-1829(99)04201-0]

The introduction of periodic arrays of artificial pinning centers into superconducting samples has been shown to give rise to different kinds of vortex behavior[1–4] that is not observed in the presence of random pinning, e.g., due to material disorder or irradiation damage. Commensurability effects between the pin array and the vortex lattice lead to greatly enhanced pinning and critical currents at a ''matching'' value of the magnetic induction, $B_1 = \mu_0 H_1$, for which the intervortex distance a_v equals the period of the pin array d. At this value of B, exactly one vortex resides on each pin site. Any additional vortex generated by increasing the applied field will be accommodated either as a multiple flux quantum on a pin site or as an interstitial vortex residing in the superconducting material between the periodic pin sites. For a square array, $H_1 = \Phi_0/d^2$. The stability of various interstitial vortex arrangements,[5] noise patterns and hysteresis in the I-V characteristics, finite transverse critical currents of the moving vortex system, and characteristic narrow-band noise spectra have been predicted in recent numerical studies.[6]

Several types of periodic pinning centers have been studied including microholes,[1,2] thickness modulations,[4] and magnetic dots.[3] Here we investigate the effect of lattices of microholes on the vortex dynamics of vanadium films. The characteristic size of microholes should be of the same order as the superconducting coherence length $\xi(T) = \xi_0/(1 - T/T_c)^{1/2}$ (≈ 100 nm for vanadium at temperatures close to T_c) to provide effective flux-line (FL) pinning. This imposes limitations on the fabrication technique used to make such pinning centers, and up to now, only electron beam lithography (EBL) has been employed to perform this task.[1–4] The main drawback to EBL is that it is too slow and expensive to pattern areas large enough necessary for useful sample fabrication. An attractive alternative method for patterning films developed in the present study is based on laser interferometric lithography (IL).[7–12]

The main principle of IL is shown in Fig. 1. A silicon wafer with a 100-nm thick, thermally grown SiO_2 insulating layer is spin coated with a $\sim$0.8 μm thick novolak-based I-line photoresist (Shipley-510). The wafer is exposed to the interference pattern created by two coherent, equal-intensity plane waves derived from a single laser source ($\lambda = 364$ nm from a TEM_{00} Ar-ion laser). The plane waves are symmetrically incident about the wafer normal with the separation angle of 2θ. A simple 90° Fresnel mirror arrangement provides stability for these exposures without requiring an active control loop and also ensures equal intensities. The period is selected by rotating the entire assembly. The resulting aerial image is sinusoidal with a period of $\lambda/2 \sin\theta$. Two exposures with the wafer rotated by 90 yield a square array of photoresist dots. A triangular array could be formed by three exposures with 60° rotations. A post-exposure bake (hotplate, 110 °C for 60 s) is used to strengthen the resist to avoid surface-tension induced collapse on developing these high aspect ratio structures.[10] Nonlinearities in the exposure and development processes transform the sinusoidal exposure profile into nearly vertical sidewalls for the final devel-
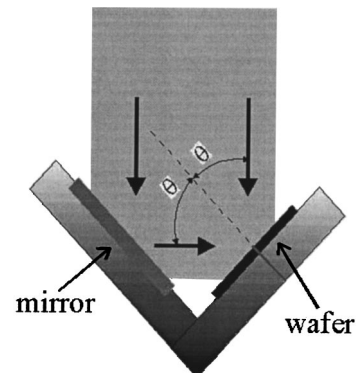
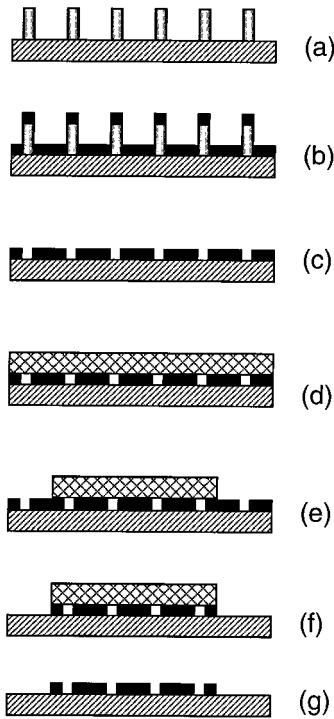FIG. 1. Schematic layout of interferometric lithography.

FIG. 2. Steps of the sample fabrication: (a) photoresist pillars 0.8 μm high, 1 μm apart on Si/SiO$_2$ substrate; (b) *e*-beam deposition of 1500 Å vanadium film; (c) liftoff of photoresist pillars. This step produces the square lattice of holes in vanadium film; (d) vanadium film with lattice of holes covered with 1.8 μm thick 1818 Microposit photoresist and prebaked; (e) photoresist layer is patterned by UV lithography; (f) using the patterned photoresist layer as a mask the final structures are produced: squares for magnetization and bridges for transport measurements [Fig. 3(c)]; (g) stripping of photoresist.

oped photoresist profile. Before development, the samples are soaked in chlorobenzene for 60 s to retard the development of the pillar tops and create an undercut photoresist structure suitable for the subsequent liftoff process. The steps of the sample fabrication are shown schematically in Fig. 2. Using *e*-beam evaporation a vanadium film is deposited onto the array of photoresist pillars, in this case a 1 μm$\times$1 μm square array with 0.4 μm pillar diameter, Fig. 2(b). After liftoff a vanadium film containing the square array of holes is obtained [Fig. 2(c)]. This film is patterned into the final structure using standart optical lithography and wet chemical or reactive ion etching [Figs. 2(d)–2(g)]. 2$\times$2 mm^2 square samples for magnetization measurements and bridges for transport measurements as shown in Fig. 3 were prepared. Au wires were attached using silver epoxy and postbaking. Part of the same substrate without photoresist pillars was used to fabricate a nonperforated reference film. dc magnetization and ac susceptibility of the sample were determined using a commercial superconducting quantum interference device magnetometer. The transport characteristics were measured on bridges such as shown in Fig. 3(c) employing dc and ac currents.

Figure 4(a) shows the temperature dependence of the resistivity and susceptibility $\chi = \chi' + i\chi''$ in a static field of 1 G for a 1500 Å thick vanadium film containing a 1$\times$1 μm^2 square lattice of holes with diameter $D = 0.4$ μm indicating a
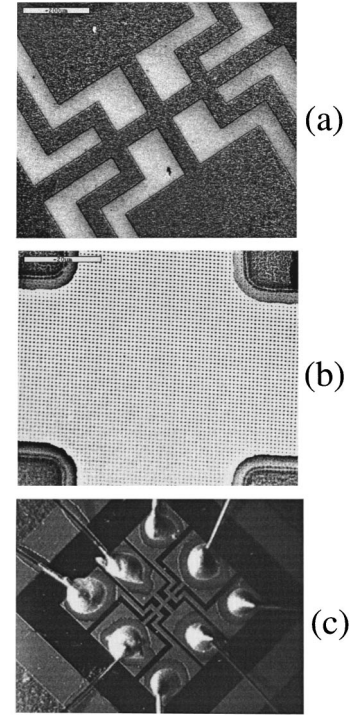

FIG. 3. (a)   SEM image of 1500 Å vanadium film with square lattice of holes (period $d = 1$ μm and diameter $D = 0.4$ μm) patterned in the bridge configuration for transport measurements.   (b) Central part of the vanadium bridge. Rows of holes parallel to the bridge sides are clearly visible. (c) Optical image of patterned vanadium film with attached Au contacts.

superconducting transition temperature $T_c \approx 4.1$ K. This value is lower than $T_c = 5.43$ K for a vanadium single crystal[13] and close to those reported for thin vanadium films.[14–16] The resistivity ρ at $T > T_c$ is 28 $\mu\Omega$ cm and close to the values reported in the literature.[17] The maxima in χ'' at $T = 4.02$ K shows that for $T > 4.02$ K the ac field with amplitude $h_0 = 0.2$ G penetrates to the center of the sample during each cycle. The introduction of the hole array causes a large increase of the magnetic response as shown in a comparison of the susceptibility of an unperforated reference sample and a perforated sample of similar size [Fig. 4(b)]. In order to facilitate the comparison between both data sets the data for the nonperforated sample have been multiplied by 20. In addition, structure in the field dependence of the susceptibility develops which will be discussed in detail below.

The two components of the complex ac susceptibility $\chi = \chi' + i\chi''$ reflect the screening current in the sample (χ') and losses (χ''), respectively. The dependences of the susceptibility on the applied dc field and on ac drive at 4.06 K are shown in Fig. 5. A sequence of sharp minima in χ' at applied fields $H_n = nH_1$ is observed, where $n = \pm 1$, ± 2, and ± 3, and $H_1 = 20.7$ G is the matching field for a $d = 1$ μm square lattice. These minima in χ' are caused by pronounced maxima in the field dependence of the critical current density occurring at the matching fields. This behavior is typically observed in samples containing periodic arrays of pinning sites.[2,3,18] For small ac-drive amplitudes h_0 ($h_0 = 0.01$ G), the *minima* in χ' correspond to *minima* in χ'', where $n = \pm 1$; ± 2 (the case of $n \pm 3$ will be discussed below). This implies that a maximum in the critical current corresponds to a mini-
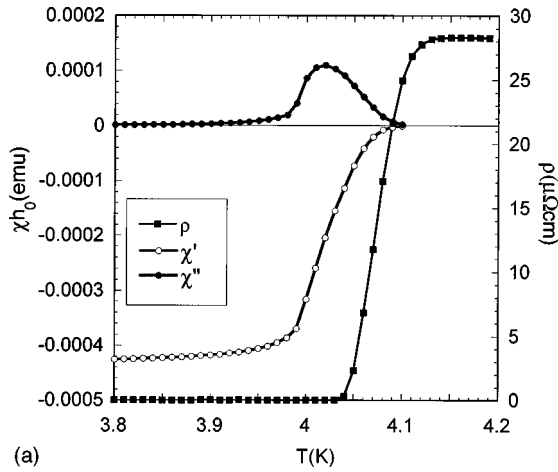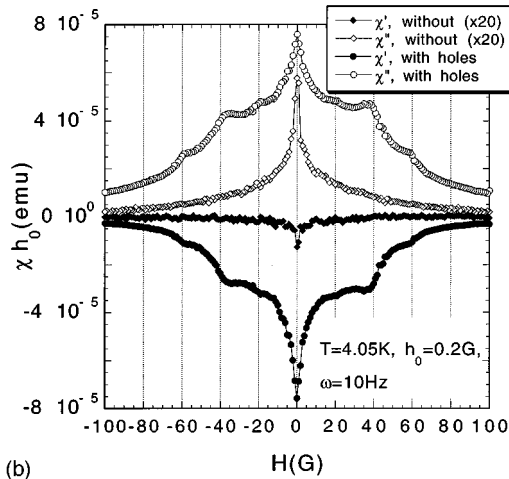
FIG. 4. (a) Temperature dependences of the susceptibility $\chi = \chi' + i\chi''$ plotted as χh_0 where $h_0 = 0.02$ G is the amplitude of the ac drive, $\omega = 10$ Hz, and temperature dependence of the resistivity ρ in a static field $H = 1$ G for a vanadium film containing a square lattice of holes. (b) Field dependences of susceptibility χh_0 for vanadium film with and without square lattice of holes at $T = 4.05$ K, $h_0 = 0.2$ G, $\omega = 10$ Hz. The dramatic effect of the hole lattice is evident.
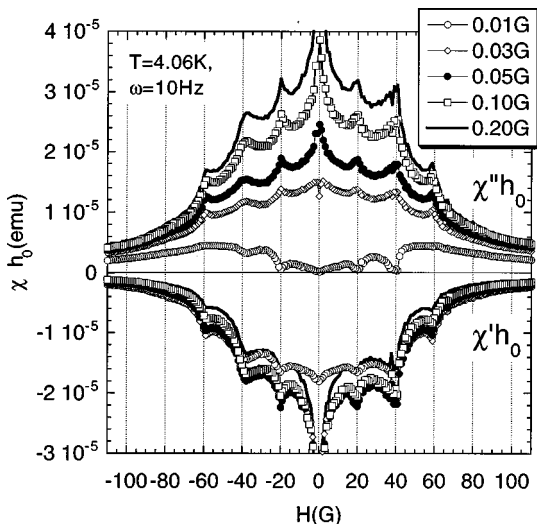

FIG. 6. Drive dependence of χh_0 at the matching field H_1, $T = 4.06$ K, $\omega = 10$ Hz. The arrow separates linear regime: $\chi' \propto h_0$, $\chi'' = 0$ for $h_0 < 0.01$ G from the nonlinear regime for higher drives. Inset shows χh_0 vs h_0 for higher drives.

mum in the ac losses, as may be expected. However, with increasing drive ($h_0 \geq 0.02$ G) the *minima* in χ'' at $H_n = nH_1$ transform into *maxima*. This behavior can be understood by realizing that the ac losses are determined by the area of *MH*-hysteresis loops that are traced out in each cycle of the ac drive.[19] At low drives the strong-pinning material effectively screens the ac field, resulting in linear response and a very narrow hysteresis loop. In contrast, sizable flux penetration occurs in the weak-pinning material, causing hysteretic losses and nonlinear response. If the ac drive is increased to such a level that flux penetration also occurs in the strong pinning then a larger hysteresis loop accompanied by higher ac losses occurs due to stronger pinning. This is indeed observed, as shown in Fig. 5. The onset of nonlinearity and enhanced ac losses in a fixed dc field of magnitude H_1 is apparent for ac amplitudes $h_0 = 0.01$ G, as shown in Fig. 6. It can be expected that with increasing $H = nH_1$ this

FIG. 5. ac susceptibility χh_0 for vanadium film with square lattice of holes for various ac drive amplitudes, $\omega = 10$ Hz, $T = 4.06$ K.
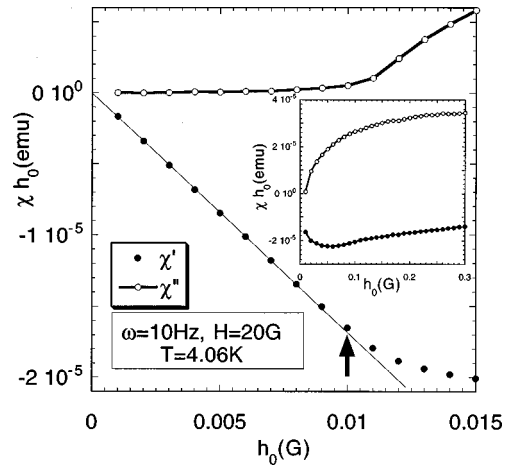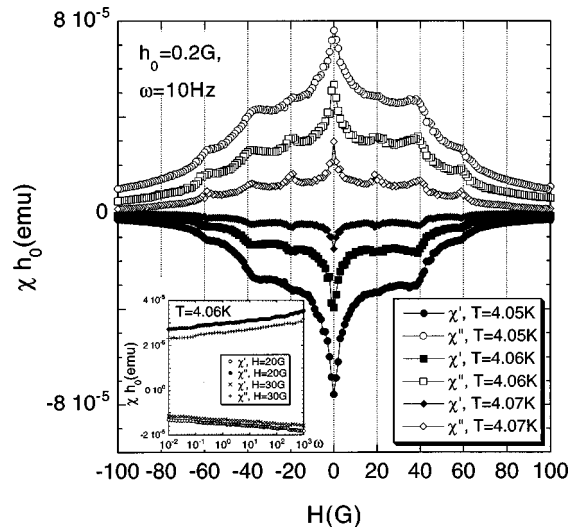

FIG. 7. Field dependence of susceptibility $\chi = \chi' + i\chi''$ for a vanadium film with square lattice of holes at different temperatures, $h_0 = 0.2$ G, $\omega = 10$ Hz. Inset: χ vs ω, $H = H_1$, $H = 3/2H_1$, $T = 4.06$ K.
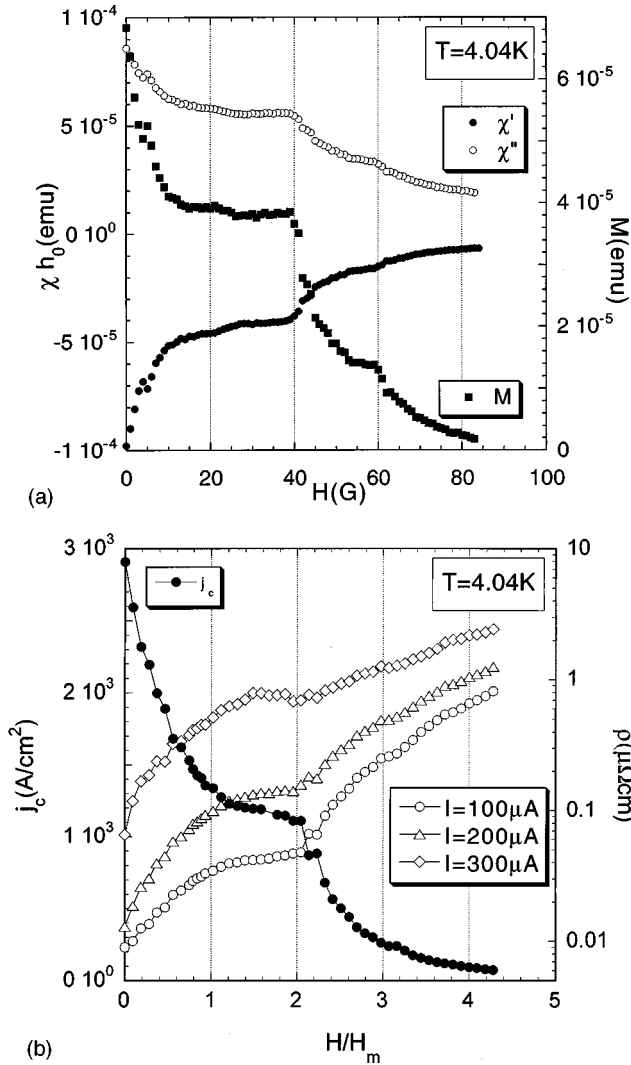
(a)

(b)

FIG. 8. (a) Field dependences of the susceptibility χh_0 and dc magnetization M for a vanadium film containing a square lattice of holes at $T=4.04$ K, $h_0=0.2$ G, $\omega=10$ Hz. (b) Field dependences of the dc critical current $I_c(H)$ (filled symbols) and magnetoresistivity $\rho(H)$ for different currents at $T=4.04$ K.

FIG. 9. Vortex configurations for: (a) $H_1>H\geqslant H_2$; (b) $H_2>H>H_3$; (c) $H_3>H\geqslant H_4$. Only ''interstitial'' vortices (open circles) are shown superimposed on the antiferromagnetic image of the sample.

onset field decreases, due to the field dependence of j_c. This suggests that the absence of dips in χ'' for $n=\pm 3$ (see Fig. 5 for $h_0=0.01$ G) is caused by a crossover into the strongly nonlinear regime at this applied field.

The magnitudes of the anomalies in $\chi(H)$ at $H_n=nH_1$ exhibit only a weak logarithmic frequency dependence observed over five decades of frequency (see inset in Fig. 7). This frequency dependence is characteristic for thermally activated creep. In an ac experiment the electric field inside the sample is largely determined by the time varying applied field. In this case the normalized flux-creep rate can be approximated[18] as $S\approx d(\ln\chi')/d(\ln\omega)$, resulting in $S=0.026$ for $H=H_1$, and $S=0.028$ for $H=1.5H_1$. These results agree well with those previously obtained in [Pb/Ge]$_n$ multilayers[2] and WGe films[18] with a square lattices of holes.

The prominence of the observed matching fields $H_n=nH_1$ is temperature dependent. In Fig. 7, we plot the ac susceptibility $\chi(H)$ for different temperatures. The anomalies in $\chi(H)$ at $H=H_n$ become less and less pronounced with decreasing temperature. At $T=4.04$ K [Fig. 8(b)] we
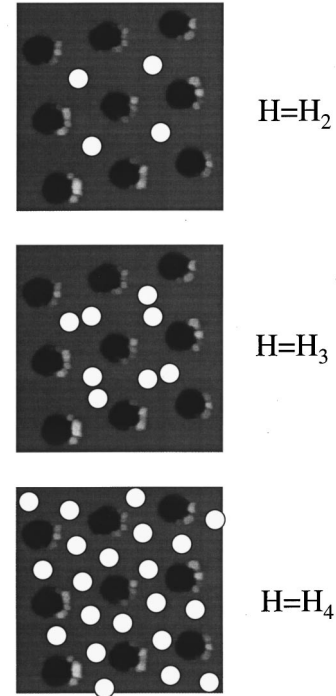
observe a well-defined anomaly only at $H=H_2$, and much weaker anomalies at H_1 and H_3. This result is supported by our dc magnetization [Fig. 8(a)] and transport measurements [Fig. 8(b)], where the resistivity $\rho(H)$ and the j_c data extracted from I-V curves show a similar behavior.

The disappearance of the anomaly at H_1 can be explained in the following way. The maximum number of vortices n_s which can be trapped in a hole as a multiquantum fluxoid is determined by a simple relation between the hole diameter D and the temperature-dependent coherence length $\xi(T)$: $n_s\approx D/4\xi(T)$.[20] For our V film, $\xi_0\approx 100$–440 Å,[13,16,17] $T_c=4.1$ K, and $D=0.4$ μm, yielding $n_s<2$ in the interval of temperature $\Delta T=T-T_c=0.1$ K, over which all our measurements were performed. This suggests that we take $n_s=1$, and assume that only one FL can occupy a hole and that a second FL will be repelled into the interstices. Based on this, we can identify the anomaly in χ at $H=H_1$ as corresponding to a configuration for which each hole has exactly one single-Φ_0 fluxoid. $H=H_2$ corresponds to the situation in which one vortex is in the hole and one vortex resides in the interstices [Fig. 9(a)]; and for $H=H_3$, we have two interstitial vortices per unit cell of the hole lattice [Fig. 9(b)]. However, the interstitial vortices are not independent from those trapped in the holes. The effective magnetic penetration depth for thin film sample of a thickness t is given by $\Lambda(T)=2\lambda(T)^2/t$.[21] For the temperature range explored here $\Lambda(T)>10$ μm which is much larger than the separation between holes indicating a strong overlap of flux lines leading to strong collective behavior. A consequence of this collective behavior is that at low temperatures the interstitial vortices are effectively ''caged'' by repulsion from vortices sitting in the holes.[22]

The temperature dependence of the ''cage potential'' was numerically calculated by Khalfin and Shapiro.[23] They predict that at lower temperatures, a pronounced minimum in free energy $F(x)$ appears at the interstitial site[23] causing strong interstitial pinning for $H \approx H_2$. However, for $H_2 < H < H_3$ a second vortex enters the interstitial region giving rise to two possible orientations of the interstitial vortex pair as shown Fig. 9(b). The activation energy for rotation between these two states is rather weak leading to an unstable vortex arrangement and suppression of the critical current for $H_2 < H < H_3$ (Fig. 8). For $H_3 < H < H_4$ interstitial vortices form a slightly distorted triangular lattice around holes. This configuration is relatively stable and changes in $I_c(H)$ and $\rho(H)$ at $H = H_3$ are not as pronounced as for $H = H_2$. Recently, these vortex configurations have been directly imaged using e-beam holography.[24]

In conclusion, we present a fabrication technique for the production of superconducting thin films containing a periodic array of pinning sites in the form of submicron holes. This technique is based on laser interferometric lithography. It allows for the fast production of large area samples without the need of joining individually written blocks as is necessary in electron beam lithography. We apply this technique to the fabrication of vanadium thin films containing a square lattice of holes with period of 1 μm and diameter of 0.4 μm. Sharp anomalies in the ac susceptibility, magnetization, and magnetoresistivity are observed at magnetic fields that correspond to the matching of the vortex lattice to the hole lattice. With increasing ac drive a characteristic change of sharp minima in the field dependence of χ'' (that is, the dissipation) to pronounced maxima is found. This transformation is explained as the crossover from linear to nonlinear vortex response. The magnitude of the anomalies in χ at the matching fields reflect the difference in stability of various vortex configurations. The sharp decrease in susceptibility and transport critical current for $H > H_2$ confirms that vortex configurations with two interstitial vortices are less stable than configurations with one or three interstitial vortices.

---

[1] A. T. Fiory, A. F. Hebard, and S. Somekh, Appl. Phys. Lett. **32**, 73 (1978).

[2] V. V. Metlushko, M. Baert, R. Jonckheere, V. V. Moshchalkov, and Y. Bruynseraede, Solid State Commun. **91**, 331 (1994); M. Baert, V. V. Metlushko, R. Jonckheere, V. V. Moshchalkov, and Y. Bruynseraede, Phys. Rev. Lett. **74**, 3269 (1995); V. V. Moshchalkov, M. Baert, V. V. Metlushko, E. Rosseel, M. J. Van Bael, K. Temst, R. Jonckheere, and Y. Bruynseraede, Phys. Rev. B **54**, 7385 (1996); V. V. Moshchalkov, M. Baert, V. V. Metlushko, E. Rosseel, M. J. Van Bael, K. Temst, Y. Bruynseraede, and R. Jonckheere, *ibid.* **57**, 3615 (1998).

[3] J. I. Martin, M. Velez, J. Nogues, and I. K. Schuller, Phys. Rev. Lett. **79**, 1929 (1997); D. J. Morgan, and J. B. Ketterson, *ibid.* **80**, 3614 (1998).

[4] A. Bezryadin and B. Pannetier, J. Low Temp. Phys. **102**, 73 (1996); A. Bezryadin, Yu. N. Ovchinnikov, and B. Pannetier, Phys. Rev. B **53**, 8553 (1996).

[5] C. Reichhardt, C. J. Olson, and F. Nori, Phys. Rev. B **57**, 7937 (1998); **58**, 6534 (1998); Phys. Rev. Lett. **78**, 2648 (1997).

[6] C. Reichhardt, J. Groth, C. J. Olson, S. B. Field, and F. Nori, Phys. Rev. B **54**, 16 108 (1996).

[7] H. Anderson, H. I. Smith, and M. L. Schattenberg, Appl. Phys. Lett. **43**, 874 (1983).

[8] S. H. Zaidi and S. R. J. Brueck, J. Vac. Sci. Technol. B **11**, 658 (1993); S. H. Zaidi, A.-S. Chu, and S. R. J. Brueck, J. Appl. Phys. **80**, 6997 (1996); X. Chen, S. H. Zaidi, S. R. J. Brueck, and D. J. Devine, J. Vac. Sci. Technol. B **14**, 3339 (1996).

[9] T. A. Savas, S. N. Shah, M. L. Schattenburg, J. M. Carter, and H. I. Smith, J. Vac. Sci. Technol. B **13**, 2732 (1996); A. Fernandez, J. Y. Decker, S. M. Herman, D. W. Phillion, D. W. Sweeney, and M. D. Perry, *ibid.* **15**, 2439 (1997).

[10] X. Chen, Z. Zhang, S. R. J. Brueck, R. A. Carpio, and J. S. Petersen (unpublished).

[11] C. O. Bozler, C. T. Harris, S. Rabe, D. D. Rathman, M. A. Hollis, and H. I. Smith, J. Vac. Sci. Technol. B **12**, 629 (1994).

[12] A. Fernandez, H. T. Nguyen, J. A. Britten, R. D. Boyd, M. D. Perry, D. R. Kania, and A. M. Hawryluk, J. Vac. Sci. Technol. B **15**, 729 (1997).

[13] S. T. Sekula and R. H. Kernohan, Phys. Rev. B **5**, 904 (1972).

[14] P. Koorevaar *et al.*, Phys. Rev. B **47**, 934 (1993).

[15] Y. Kuwasawa, E. Touma, T. Nojima, and S. Nakano, Physica B **194–196**, 2423 (1994).

[16] A. A. Teplov and M. N. Micheeva, Sov. J. Low Temp. Phys. **7**, 149 (1981).

[17] K. Kanoda, H. Mazaki, T. Yamada, N. Hosoito, and T. Shinjo, Phys. Rev. B **33**, 2052 (1986); K. Kanoda, H. Mazaki, N. Hosoito, and T. Shinjo, *ibid.* **35**, 6736 (1987).

[18] V. V. Metlushko, L. E. DeLong, M. Baert, E. Rosseel, M. J. Van Bael, K. Temst, V. V. Moshchalkov, and Y. Bruynseraede, Euerophys. Lett. **41**, 333 (1998).

[19] J. Clem, *Magnetic Susceptibility of Superconductors and Other Spin Systems*, edited by R. A. Hein (Plenum, New York, 1991).

[20] G. S. Mkrtchyan and V. V. Shmidt, Sov. Phys. JETP **34**, 195 (1972).

[21] R. D. Parks, *Superconductivity* (Marcel Dekker, New York, 1969).

[22] L. Radzihovsky, Phys. Rev. Lett. **74**, 4923 (1995).

[23] I. B. Khalfin and B. A. Shapiro, Physica C **207**, 359 (1993).

[24] K. Harada, O. Kamimura, H. Kasai, T. Matsuda, A. Tonomura, and V. V. Moshchalkov, Science **274**, 1167 (1996).